Letter

Axial Correlation Revivals and Number Factorization with Structured Random Waves

Xin Liu,[1,2,‡] Chunhao Liang,[1,2,‡] Yangjian Cai,[1,2,*] and Sergey A. Ponomarenko[3,4,†]

[1] *Shandong Provincial Engineering and Technical Center of Light Manipulation and Shandong Provincial Key Laboratory of Optics and Photonics Devices, School of Physics and Electronics, Shandong Normal University, Jinan 250014, China*

[2] *Collaborative Innovation Center of Light Manipulations and Applications, Shandong Normal University, Jinan 250358, China*

[3] *Department of Electrical and Computer Engineering, Dalhousie University, Halifax, Nova Scotia B3J 2X4, Canada*

[4] *Department of Physics and Atmospheric Science, Dalhousie University, Halifax, Nova Scotia B3H 4R2, Canada*

(Received 19 March 2023; revised 16 July 2023; accepted 26 July 2023; published 22 August 2023)

We advance a general theory of field correlation revivals of structured random wave packets, composed of superpositions of propagation invariant modes, at pairs of planes transverse to the packet propagation direction. We derive an elegant analytical relation between the normalized intensity autocorrelation function of the thus structured paraxial light fields at a pair of points on an optical axis of the system and an incomplete Gauss sum, thereby establishing a fundamental link between statistical optics and number theory. We propose and experimentally implement a simple robust analog random wave computer that can efficiently decompose numbers into prime factors.

DOI: 10.1103/PhysRevApplied.20.L021004

A spectacular self-imaging effect, first experimentally discovered by Talbot [1] and later theoretically explained by Lord Rayleigh [2], occurs whenever a one-dimensional spatially periodic structure is illuminated by a freely propagating paraxial optical field. As was shown by Rayleigh [2], the periodic field pattern formed by the structure undergoes periodic axial revivals at distances that are multiple integers of the Talbot length, $z_T = 2d^2/\lambda$, where d is a spatial period of the field pattern at the source and λ is the wavelength of light. To date, the classic Talbot-like revivals have been extensively studied for coherent and random optical waves in free space [3–6], linear graded media [7], and nonlinear optical systems [8]. Moreover, space-time duality [9] implies the existence of a temporal analogue of the spatial Talbot effect for a periodic train of optical pulses propagating in a dispersive fiber [10–12]. The spatial and temporal Talbot effects have found numerous applications in x-ray imaging [13], optical metrology, and spectroscopy [14], as well as, most recently, in temporal cloaking [15]. Thanks to a mathematical analogy between the paraxial wave equation in optics and the Schrödinger equation in quantum mechanics, Talbot recurrences have been explored in atom optics [16–18] and Bose-Einstein condensates [19], as well as in the C_{70} fullerene molecule [20] and Rydberg wave packet [21] interferometry.

Lately, wave pattern revivals of structured fields have attracted interest [22] and novel manifestations of spatial [23] and temporal [24], as well as space-time [25] Talbot effects have been discovered for space-time wave packets for which spatial and temporal frequencies of individual monochromatic waves, composing the packets, are tightly coupled [26]. Further, aperiodic field correlations of an uncorrelated superposition of two Bessel beams at pairs of planes, transverse to the beam propagation direction in free space, have been shown to undergo perfect revivals over the Talbot distance [27].

Here, we develop a general theory of axial correlation revivals of structured random waves composed of superpositions of diffraction-free modes of any kind. Our theory enables us to derive a remarkably simple analytical relation between the normalized intensity autocorrelation function of structured paraxial random light fields at a pair of points on an optical axis of the system and an incomplete Gauss sum, thereby establishing a fundamental link between statistical optics and number theory. We employ the discovered link to advance and experimentally implement an efficient protocol to decompose

*yangjian_cai@163.com
†serpo@dal.ca
‡These authors contributed equally to this work

even fairly large numbers into prime factors using random light.

Number factorization plays a prominent role in network systems and cyber security [28], as well as in optimization [29,30]. It has also become a crucial ingredient of a host of promising physics-based protocols for information encoding [31], optical encryption [32], and all-optical machine learning [33]. Moreover, intriguing prime number links have emerged to quantum ladder states of many-body systems [34] and multifractality of light in photonic arrays undergirded by algebraic number theory [35].

Although quantum algorithms have enabled seminal advances in number factorization [36], the application of quantum mechanics to this problem requires the implementation of a complex quantum Hamiltonian, such that factoring even relatively small numbers can run into unexpected difficulties [[37]]. In addition, the entanglement of a large number of qubits is susceptible to pernicious decoherence effects [38]. Hence, alternatives have been sought that rely on the physics of classical superpositions of coherent waves [39–41]. The latter, however, are very sensitive to external noise. In contrast, our protocol involves classical random waves, which are robust against noise [42,43], and the protocol capacity is only limited by the pixel size of a spatial light modulator (see the Supplemental Material [44]).

We consider a random wave packet and an associated ensemble of scalar random fields $\{U\}$. In the space-frequency representation, the field of each ensemble realization can be expressed as

$$U(\mathbf{r},z,\omega)=\sum_{\nu}a_{\nu}\Psi_{\nu}(\mathbf{r},z,\omega), \tag{1}$$

where z and $\mathbf{r}$ are the axial coordinate along and radius vector in the plane transverse to the packet propagation direction, respectively. Further, $\{a_{\nu}\}$ is a set of uncorrelated random amplitudes that obey the second-order statistics as

$$\langle a_{\nu}^{*}a_{\nu'}\rangle=\lambda_{\nu}\delta_{\nu\nu'}. \tag{2}$$

Here, the angle brackets represent ensemble averaging and $\{\lambda_{\nu}\geq 0\}$ specify powers of individual modes $\{\Psi_{\nu}\}$.

We now specify to a particular class of spatial modes,

$$\Psi_{\nu}(\mathbf{r},z,\omega)=\psi_{\nu}(\mathbf{r},\omega)e^{i\beta_{\nu}(\omega)z}, \tag{3}$$

and drop the irrelevant frequency variable ω hereafter. We can infer from Eq. (3) that each mode, characterized by a propagation constant β_{ν}, defies diffraction. It follows that $\{\Psi_{\nu}\}$ are either modes of a chaotic multimode (optical, acoustical, or matter) waveguide or $\{\Psi_{\nu}\}$ belong to a special class of nondiffracting modes of the Helmholtz equation in free space.

Next, we define the cross-spectral density of the ensemble at a pair of transverse planes $z_1=\text{const}$ and $z_2=\text{const}$ as

$$W(\mathbf{r}_1,z_1;\mathbf{r}_2,z_2)=\langle U^{*}(\mathbf{r}_1,z_1)U(\mathbf{r}_2,z_2)\rangle. \tag{4}$$

On substituting from Eqs. (1) through (3) into Eq. (4), we can readily conclude that

$$W(\mathbf{r}_1,\mathbf{r}_2,\Delta z)=\sum_{\nu}\lambda_{\nu}\psi_{\nu}^{*}(\mathbf{r}_1)\psi_{\nu}(\mathbf{r}_2)e^{i\beta_{\nu}\Delta z}, \tag{5}$$

where $\Delta z=z_2-z_1$. The analysis of Eq. (5) reveals that the cross-spectral density of the field in any given transverse plane $z_1=z_2=\text{const}$ remains the same due to the propagation invariance of the modes. Yet even uncorrelated modes manifest axial dynamics due to the interference of phasors $e^{i\beta_{\nu}\Delta z}$ when correlations in different transverse planes are examined. In particular, if the propagation constant is proportional to a polynomial in ν with integer coefficients, $\beta_{\nu}=(2\pi/z_r)\sum_s c_s\nu^s$, $c_s\in\mathcal{Z}$, and $s\in\mathcal{N}$, $W(\mathbf{r}_1,\mathbf{r}_2,\Delta z)$ self-images over multiples of a characteristic revival distance z_r. This is a generic feature of the axial correlations of wave fields composed of discrete diffraction-free modes.

Let us now focus on structured random sources generating uncorrelated superpositions of the so-called dark or antidark (DAD) diffraction-free beams of light, featuring dark notches or bright bumps against an incoherent background [45,46]. Instructively, the DAD beams have been recently shown to maintain structural stability even in random media [47].

We show (for details, see the Supplemental Material [44]) that the cross-spectral density of the DAD beam superposition ensemble at a given radial position r in any pair of transverse planes is given, up to an immaterial constant and an overall phase factor, by the expression

$$W_{\mathrm{DAD}}(\mathbf{r},\Delta z)\propto\sum_{m=1}^{M}[1\mp J_0(4\pi mr/d)]e^{-2\pi im^2\Delta z/z_T}, \tag{6}$$

where $J_0(x)$ is a Bessel function of the first kind and order zero and $-$ $(+)$ on the right-hand side of the equation corresponds to a superposition of dark (antidark) beams, respectively.

We display the average intensity and the magnitude of $W_{\mathrm{DAD}}(r,\Delta z)$ in Fig. 1 for antidark beams [Figs. 1(a) and 1(c)] and dark beams [Figs. 1(b) and 1(d)]. We can observe in the figure that while the average intensity remains propagation invariant, the two-plane correlations exhibit, in general, intricate dynamics revealing perfect periodic revivals. Specifically, we can infer from Eq. (6) and observe in Figs. 1(c) and 1(d) that aperiodic DAD field correlations are perfectly reproduced at pairs of axial distances separated by multiple Talbot lengths. At the same time, two-point angular correlations of the ensemble of DAD beam

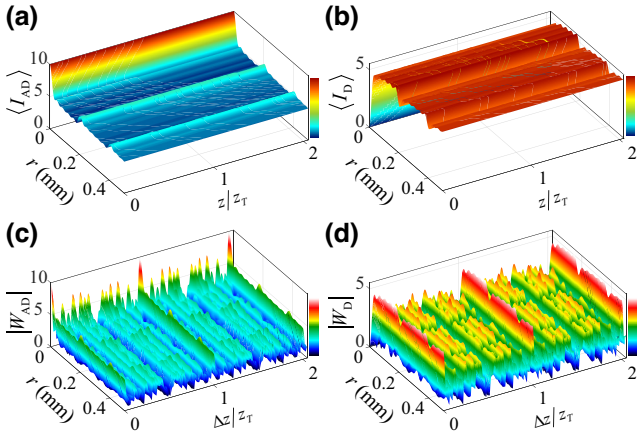

FIG. 1. The (a),(b) (propagation-invariant) average intensity and (c),(d) magnitude of the cross-spectral density of an ensemble of (a),(c) antidark-beam and (b),(d) dark-beam superpositions, evaluated at a pair of points with coordinates $(\mathbf{r}, z_1)$ and $(\mathbf{r}, z_2)$, $\Delta z = z_2 - z_1$, using Eq. (6) with $M = 5$ and $d = 0.4$ mm. At the multiples of the classic Talbot distance z_T, aperiodic DAD-field correlations are perfectly reproduced.

superpositions show even more intriguing Talbot carpets, replete with full and fractional Talbot revivals (see the Supplemental Material [44]). Further, we can introduce the second-order degree of coherence of the fields [48] at a pair of points $(\mathbf{r}, z_1)$ and $(\mathbf{r}, z_1 + \Delta z)$ as

$$\mu_{\mathrm{DAD}}(\mathbf{r}, \Delta z) = \frac{W_{\mathrm{DAD}}(\mathbf{r}, \Delta z)}{W_{\mathrm{DAD}}(\mathbf{r}, 0)}. \tag{7}$$

It follows at once from Eqs. (6) and (7) that provided $\Delta z = nz_T$, $n \in \mathcal{N}$, the fields are perfectly coherent at all pairs of points parallel to the optical axis in the transverse planes separated by multiple revival distances, $|\mu_{\mathrm{DAD}}(\mathbf{r}, nz_T)| = 1$. We can infer from Eqs. (5) and (7) that this is a statistical signature of correlation revivals of wave packets composed of any propagation-invariant modes $\{\Psi_v\}$.

The presence of a quadratic exponential factor in Eq. (6) hints at the possibility of employing correlations of structured random light fields to factor numbers. Indeed, we can establish a link between the normalized intensity autocorrelation function of the peak intensities of antidark (AD) beams I_{AD}, evaluated at different positions along the optical axis, and an incomplete Gauss sum of number theory. To this end, we define the former as

$$g^{(2)}_{\mathrm{AD}}(0, \Delta z) = \frac{\langle I_{\mathrm{AD}}(0, z + \Delta z) I_{\mathrm{AD}}(0, z)\rangle}{\langle I_{\mathrm{AD}}(0, z)\rangle^2} \tag{8}$$

and the latter as

$$\mathcal{G}^{(M)}_N(p) = \frac{1}{M} \sum_{m=1}^{M} e^{-2\pi i m^2 N/p} \tag{9}$$

and derive the following fundamental relation (for details, see the Supplemental Material [44]):

$$|\mathcal{G}^{(M)}_N(p)|^2 = g^{(2)}_{\mathrm{AD}}(0, z_T N/p) - 1. \tag{10}$$

In Eqs. (9) and (10), N is a number that we seek to factor and p, $p \in \mathcal{N}$, are trial prime integers that may or may not be factors of N. The left-hand side of Eq. (10) equals unity whenever p is a factor of N and it oscillates rapidly, taking on small values otherwise. Remarkably, we have revealed a link between a number-theoretic quantity, the incomplete Gauss sum, and a fundamental measurable quantity of statistical optics, the intensity autocorrelation function of light fields. It follows that we can sample $\mathcal{G}^{(M)}_N$ at discrete points by evaluating, from experimental data, the (normalized) intensity-intensity correlations of light at pairs of points separated by the interval $\Delta z = z_T N/p$ along the optical axis of the system.

Next, we validate the proposed protocol by carrying out a number factorization experiment. In our experiment, a collimated linearly polarized, quasi-monochromatic beam of carrier wavelength $\lambda = 632.8$ nm, emitted by a He-Ne laser, illuminates a phase-only spatial light modulator (SLM) (Meadowlark Optics, 1920×1200 8 μm^2 pixels). To structure random light beams, we encode the desired field distributions into holograms using complex amplitude encoding. The sought beams are then associated with the first diffracted order from the SLM; we refresh the speckle patterns by refreshing the holograms (for further details, see the Supplemental Material [44]).

In Fig. 2, we present two typical ensemble representations (speckle patterns of instantaneous intensities) of light at the two axial distances corresponding to $p = 3$ (top row, p being a factor of N) and $p = 4$ (bottom row), with $M = 5$ and $N = 1155$. We average over an ensemble of 2000 speckle patterns to evaluate the normalized intensity autocorrelation functions $g^{(2)}_{\mathrm{AD}}(\mathbf{r}, z_T N/p)$ with the help of Eq. (S11) in the Supplemental Material [44]. We can show analytically (see the Supplemental Material [44]) that whenever $N = np$, $n \in \mathcal{N}$, $g^{(2)}_{\mathrm{AD}}(\mathbf{r}, Nz_T/p) = 2$ at any transverse location $\mathbf{r}$, implying that $|\mathcal{G}^{(M)}_N(p)|^2 = 1$ in Eq. (10). This conclusion is well supported by our experimental results of Fig. 2(c), wherein slight deviations from the theory can be further suppressed by increasing the size of the ensemble.

To demonstrate the capability of our protocol to factor large numbers, we show theoretical and experimental results, corresponding to the left- and right-hand sides of Eq. (10), respectively, as functions of p in Fig. 3: these are marked by red squares (theory) and blue dots (experiment). In Fig. 3(a), a relatively small number to be factorized is comprised of four adjacent primes ($N = 1155 = 3 \times 5 \times 7 \times 11$), whereas Fig. 3(b) exhibits the factorization of a large number composed of prime factors that are far apart

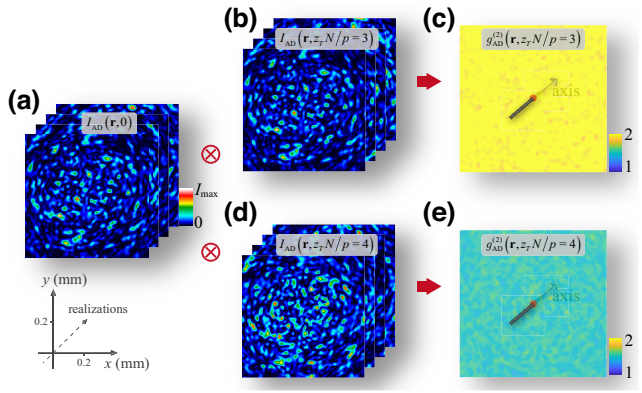

FIG. 2. (a),(b),(d) Speckle patterns (the instantaneous intensity) of the structured random light (AD beam with $M = 5$ and $N = 1155$). (c),(e) The resulting normalized intensity autocorrelation functions. We choose $p = 3$ in (a)–(c) and $p = 4$ in (a), (d), and (e), respectively. In the former case, p is a factor of N, whereas this is not the case in the latter situation. The normalized intensity autocorrelation functions $g^{(2)}_{\mathrm{AD}}(\mathbf{r}, z_T N/p)$ in (c) and (e) are evaluated by averaging over an ensemble of 2000 speckle patterns with the aid of Eq. (S11) of the Supplemental Material [44], which reduces to Eq. (8) on the optical axis.

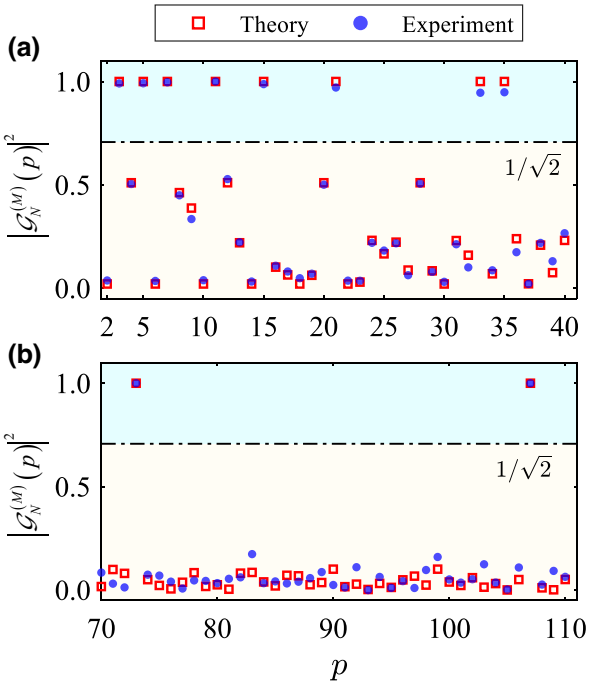

FIG. 3. Experimental number factorization with structured random light beams. The relevant parameters are as follows: (a) $N = 1155 = 3 \times 5 \times 7 \times 11$ and $M = 5$; (b) $N = 570\,203 = 73^2 \times 107$ and $M = 20$. The theoretical and experimental results are obtained from Eqs. (9) and (10), respectively.

from one another: $N = 570\,203 = 73^2 \times 107$. The results clearly demonstrate that $|\mathcal{G}^{(M)}_N(p)|^2$ attains unity (within the experimental accuracy) for all prime factors of N. Further, the factors and nonfactors of N are clearly discriminated by the threshold value of $1/\sqrt{2}$, as anticipated [49].

Next, to ensure the accuracy of number factorization, we demonstrate that our protocol is able to detect spurious factors, the ghost factors, such that the magnitude of the incomplete Gauss sum can attain values close to unity. To suppress any ghost factor below the threshold value, the magnitude of M must be chosen judiciously. Previous work on number factorization with incomplete Gauss sums suggests the criterion $M \approx 0.659\sqrt[4]{N}$ for a given N [49]. To illustrate ghost number suppression in our protocol, we focus on a large number, $N = 186\,623 = 431 \times 433$, composed of two twin primes, and analyze the ghost factor 432. In Fig. 4, we display the theoretical and experimental results for $|\mathcal{G}^{(M)}_{(431\times433)}(432)|^2$ as functions of M. We can infer from the figure that both curves fall off with M, exhibiting slight oscillations at their large M tails. The curves intersect the horizontal line $|\mathcal{G}|^2 = 1/\sqrt{2}$ at $M = 11.1$, implying that the ghost factors are suppressed provided that $M \geq 12$. To verify this conclusion and impart intuition, we also plot $|\mathcal{G}^{(12)}_{(431\times433)}|^2$ as a function of p evaluated for $M = 12$ in the inset to the figure. We can readily conclude from the inset that the ghost factor 432 is clearly suppressed and that only 431 and 433 are eligible prime factors of 186 623.

In conclusion, we have advanced a general theory of axial correlation revivals of structured random waves composed of superpositions of propagation-invariant modes. We have employed the developed theory to establish a fundamental link between statistical optical physics and number theory and have proposed and demonstrated a

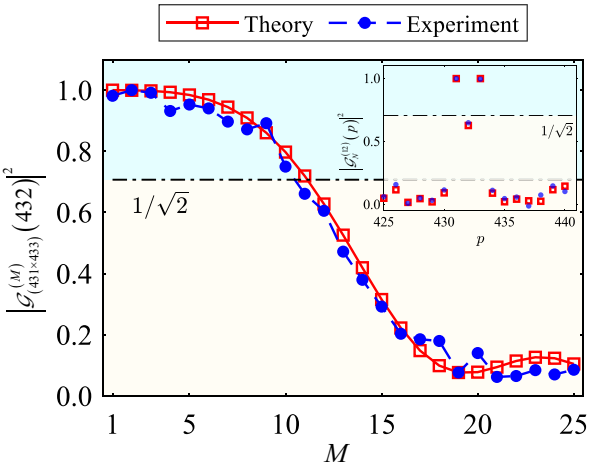

FIG. 4. Experimental analysis of ghost-factor $p = 432$ suppression in the factorization of $N = 186\,623 = 431 \times 433$ as a function of the number of modes M. The inset shows the experimental results of factoring $N = 186\,623$ with $M = 12$.

protocol to decompose numbers into prime factors using random light. It is worth noting that all previously reported classical physics inspired number factorization techniques have relied on coherent superpositions of waves [39–41,50]. The strict control of wave phases has been achieved by employing carefully controlled sequences of nuclear spins [39], cold atoms [40], or femtosecond optical pulses [41], which, in turn, has called for sophisticated experimental apparatuses [39–41] and cryogenic temperatures [40]. In contrast, our protocol requires only commercially available table-top optical components and it employs cw random light, which is quite robust to source or environmental noise. It is then noteworthy that without making any attempt to optimize our procedure, we have been able to factor numbers as large as $N = 570\,203$ which is, at least, on par with current achievements by protocols based on NMR ($N = 157\,573$) [39] and cold atoms ($N = 263\,193$) [40] and an order of magnitude larger than the greatest number ($N = 19\,043$) that has been factorized with coherent sequences of femtosecond pulses to date [41]. Moreover, the largest number amenable to factorization with coherent cw light beams has been a mere 27 [50], so that our protocol enables an improvement by 4 orders of magnitude. As a matter of fact, the upper bound on the number that can be decomposed into primes with our protocol is set by the pixel size of the commercial SLM employed in our experiment (for further details, see the Supplemental Material [44]). As the emerging nanophotonics technology for structuring random light [51] matures, we fully anticipate further rapid advances in this direction. In addition, we are confident that similar number factorization protocols can be developed to operate with noisy acoustical or matter waves to be structured with the aid of appropriate metasurfaces [52,53].

Acknowledgments—We acknowledge financial support from the National Key Research and Development Program of China (Grants No. 2022YFA1404800 and No. 2019YFA0705000), the National Natural Science Foundation of China (Grants No. 12004220, No. 11974218, No. 12192254, and No. 92250304), the Regional Science and Technology Development Project of the Central Government (Grant No. YDZX20203700001766), the China Postdoctoral Science Foundation (Grant No. 2022T150392), and the Natural Sciences and Engineering Research Council of Canada (Grant No. RGPIN-2018-05497).

[1] H. F. Talbot, Facts relating to optical science, no. IV, Philos. Mag. **9**, 401 (1836).
[2] Lord Rayleigh, On copying diffraction gratings and on some phenomenon connected therewith, Philos. Mag. **11**, 196 (1881).
[3] J. T. Winthrop and C. R. Worthington, Theory of Fresnel images, I. Plane periodic objects in monochromatic light, J. Opt. Soc. Am. **55**, 373 (1965).
[4] W. D. Montgomery, Self-imaging objects of infinite aperture, J. Opt. Soc. Am. **57**, 772 (1967).
[5] M. Berry and S. Klein, Integer, fractional and fractal Talbot effects, J. Mod. Opt. **43**, 2139 (1996).
[6] T. Saastamoinen, J. Tervo, P. Vahimaa, and J. Turunen, Exact self-imaging of transversely periodic fields, J. Opt. Soc. Am. A **21**, 1424 (2004).
[7] S. A. Ponomarenko, Self-imaging of partially coherent light in graded-index media, Opt. Lett. **40**, 566 (2015).
[8] Y. Zhang, J. Wen, S. Zhu, and M. Xiao, Nonlinear Talbot Effect, Phys. Rev. Lett. **104**, 183901 (2010).
[9] B. H. Kolner, Space-time duality and the theory of temporal imaging, IEEE J. Quantum Electron. **30**, 1951 (1994).
[10] T. Jannson and J. Jannson, Temporal self-imaging effect in single-mode fibers, J. Opt. Soc. Am. **71**, 1373 (1981).
[11] P. Andrekson, Linear propagation of optical picosecond pulse trains over oceanic distances, Opt. Lett. **18**, 1621 (1993).
[12] F. Mitschke and U. Morgner, The temporal Talbot effect, Opt. Photonics News **9**, 45 (1998).
[13] T. Weitkamp, B. Nöhammer, A. Diaz, C. David, and E. Ziegler, X-ray wavefront analysis and optics characterization with a grating interferometer, Appl. Phys. Lett. **86**, 054101 (2005).
[14] J. Wen, Y. Zhang, and M. Xiao, The Talbot effect: Recent advances in classical optics, nonlinear optics, and quantum optics, Adv. Opt. Photonics **5**, 83 (2013).
[15] B. Li, X. Wang, J. Kang, Y. Wei, T. Yung, and K. K. Y. Wong, Extended temporal cloak based on the inverse temporal Talbot effect, Opt. Lett. **42**, 767 (2017).
[16] J. F. Clauser and S. Li, Talbot–von Lau atom interferometry with cold slow potassium, Phys. Rev. A **49**, R2213 (1994).
[17] M. S. Chapman, C. R. Ekstrom, T. D. Hammond, J. Schmiedmayer, B. E. Tannian, S. Wehinger, and D. E. Pritchard, Near-field imaging of atom diffraction gratings: The atomic Talbot effect, Phys. Rev. A **51**, R14 (1995).
[18] S. Wu, E. Su, and M. Prentiss, Demonstration of an Area-Enclosing Guided-Atom Interferometer for Rotation Sensing, Phys. Rev. Lett. **99**, 173201 (2007).
[19] L. Ding, E. W. Hagley, J. Denschlag, J. E. Simsarian, M. Edwards, C. W. Clark, K. Helmerson, S. L. Rolston, and W. D. Phillips, Temporal, Matter-Wave-Dispersion Talbot Effect, Phys. Rev. Lett. **83**, 5407 (1999).
[20] B. Brezger, L. Hackermuller, S. Uttenhaler, J. Petschinka, M. Arndt, and A. Zeilinger, Matter-Wave Interferometer for Large Molecules, Phys. Rev. Lett. **88**, 100404 (2002).
[21] J. Parker and C. R. Stroud Jr., Coherence and Decay of Rydberg Wave Packets, Phys. Rev. Lett. **56**, 716 (1986).
[22] B. Pinheiro da Silva, V. A. Pinillos, D. S. Tasca, L. F. Oxman, and A. Z. Khoury, Pattern Revivals from Fractional Gouy Phases in Structured Light, Phys. Rev. Lett. **124**, 033902 (2020).
[23] M. Yessenov, L. A. Hall, S. A. Ponomarenko, and A. F. Abouraddy, Veiled Talbot Effect, Phys. Rev. Lett. **125**, 243901 (2020).
[24] L. A. Hall, S. A. Ponomarenko, and A. Abouraddy, Temporal Talbot effect in free space, Opt. Lett. **46**, No. 3107 (2021).
[25] L. A. Hall, M. Yessenov, S. A. Ponomarenko, and A. F. Abouraddy, The space-time Talbot effect, APL Photonics **6**, 056105 (2021).

[26] M. Yessenov, L. A. Hall, K. L. Schepler, and A. F. Abouraddy, Space-time wave packets, Adv. Opt. Photonics **14**, 455 (2022).
[27] J. S. Rodriguez, E. J. S. Fonseca, and A. J. Jesus-Silva, Talbot effect with partially coherent interfering Bessel beams, Appl. Opt. **57**, 3186 (2018).
[28] N. Koblitz, *A Course in Number Theory and Cryptography,* (Springer, New York, 1994).
[29] R. E. Steuer, *Multiple Criteria Optimization: Theory, Computation and Application* (Wiley, New York, 1986).
[30] H. Li, Y. Huang, S. Fang, and W. Kuo, A prime-logarithmic method for optimal reliability design, IEEE Trans. Reliab. **70**, 146 (2021).
[31] H. Li, S. Fang, B. M. T. Lin, and W. Kuo, Unifying colors by primes, Light Sci. Appl. **12**, 32 (2023).
[32] L. Kong, W. Zhang, P. Li, X. Guo, J. Zhang, F. Zhang, J. Zhao, and X. Zhang, High capacity topological coding based on nested vortex knots and links, Nat. Commun. **13**, 2705 (2022).
[33] X. Lin, Y. Rivenson, N. T. Yardimci, M. Veli, Y. Luo, M. Jarrahi, and A. Ozcan, All-optical machine learning using diffractive deep neural networks, Science **361**, 1004 (2018).
[34] G. Mussardo, A. Trombettoni, and Z. Zhang, Prime Suspects in a Quantum Ladder, Phys. Rev. Lett. **125**, 240603 (2020).
[35] F. Sgrignuoli, S. Gorsky, W. A. Britton, R. Zhang, F. Riboli, and L. Dal Negro, Multifractality of light in photonic arrays based on algebraic number theory, Commun. Phys. **3**, 106 (2020).
[36] L. M. K. Vandersypen, M. Steffen, G. Breyta, C. S. Yannoni, M. H. Sherwood, and I. L. Chuang, Experimental realization of Shor's quantum factoring algorithm using nuclear magnetic resonance, Nature (London) **414**, 883 (2001).
[37] A. Dash, D. Sarmah, B. K. Behera, and P. K. Panigrahi, Exact search algorithm to factorize large biprimes and a triprime on IBM quantum computer, ArXiv:1805.10478v2 (2018).
[38] M. A. Nielsen and I. L. Chuang, *Quantum Computation and Quantum Information* (Cambridge University Press, Cambridge, 2000).
[39] M. Mehring, T. Müller, I. Sh. Averbukh, W. Merkel, and W. P. Schleich, NMR Experiment Factors Numbers with Gauss Sums, Phys. Rev. Lett. **98**, 120502 (2007).
[40] M. Gilowski, T. Wendrich, T. Müller, Ch. Jentsch, W. Ertmer, E. M. Rasel, and W. P. Schleich, Gauss Sum Factorization with Cold Atoms, Phys. Rev. Lett. **100**, 030201 (2008).
[41] D. Bigourd, B. Chatel, W. P. Schleich, and B. Girard, Factorization of Numbers with the Temporal Talbot Effect: Optical Implementation by a Sequence of Shaped Ultrashort Pulses, Phys. Rev. Lett. **100**, 030202 (2008).
[42] Z. Huang, Y. Chen, F. Wang, S. A. Ponomarenko, and Y. Cai, Measuring Complex Degree of Coherence of Random Light Fields with Generalized Hanbury Brown and Twiss Experiment, Phys. Rev. Appl. **13**, 044042 (2020).
[43] D. Peng, Z. Huang, Y. Liu, Y. Chen, F. Wang, S. A. Ponomarenko, and Y. Cai, Optical coherence encryption with structured random light, PhotoniX **2**, 1 (2021).
[44] See the Supplemental Material at http://link.aps.org/supplemental/10.1103/PhysRevApplied.20.L021004 for detailed theoretical analysis and the discussion of our experimental protocol and its capabilities, including Refs. [54–60].
[45] S. A. Ponomarenko, W. Huang, and M. Cada, Dark and antidark diffraction-free beams, Opt. Lett. **32**, 2508 (2007).
[46] X. Zhu, F. Wang, C. Zhao, Y. Cai, and S. A. Ponomarenko, Experimental realization of dark and antidark diffraction-free beams, Opt. Lett. **44**, 2260 (2019).
[47] Z. Xu, X. Liu, Y. Cai, S. A. Ponomarenko, and C. Liang, Structurally stable beams in the turbulent atmosphere: Dark and antidark beams on incoherent background [Invited], J. Opt. Soc. Am. A **39**, C51 (2022).
[48] L. Mandel and E. Wolf, *Optical Coherence and Quantum Optics* (Cambridge University Press, Cambridge, 1995).
[49] M. Štefaňák, W. Merkel, W. P. Schleich, D. Haase, and H. Maier, Factorization with Gauss sums: Scaling properties of ghost factors, New J. Phys. **9**, 370 (2007).
[50] K. Pelka, J. Graf, T. Mehringer, and J. von Zanthier, Prime number decomposition using the Talbot effect, Opt. Express **26**, 15009 (2018).
[51] L. Liu, W. Liu, F. Wang, H. Cheng, D. Y. Choi, J. Tian, Y. Cai, and S. Chen, Spatial coherence manipulation on the disorder-engineered statistical photonic platform, Nano Lett. **22**, 6342 (2022).
[52] B. Assouar, B. Liang, Y. Wu, Y. Li, J-C. Cheng, and Y. Jing, Acoustic metasurfaces, Nat. Rev. Mater. **3**, 460 (2018).
[53] W. Xiao and C. Huang, Metasurfaces for de Broglie waves, Phys. Rev. B **104**, 245429 (2021).
[54] I. S. Gradstein and I. M. Ryzhik, *Tables of Integrals, Series and Products* (Academic Press, New York, 1980).
[55] S. A. Ponomarenko and E. Wolf, Coherence properties of light in Young's interference pattern formed with partially coherent light, Opt. Commun. **170**, 1 (1999).
[56] G. W. Goodman, *Statistical Optics* (Wiley, New York, 2015).
[57] K. Ireland and M. Rosen, *A Classical Introduction to Modern Number Theory*, Graduate Texts in Mathematics (Springer, New York, 1990).
[58] C. Rosales-Guzmán and A. Forbes, *How to Shape Light with Spatial Light Modulators* (SPIE, Washington, 2017).
[59] H. Li, Z. Yu, Q. Zhao, Y. Luo, S. Cheng, T. Zhong, C. M. Woo, H. Liu, L. Wang, Y. Zheng, and P. Lai, Learning-based super-resolution interpolation for sub-Nyquist sampled laser speckles, Photonics Res. **11**, 631 (2023).
[60] Y. Piederrière, J. Cariou, Y. Guern, B. Le Jeune, G. Le Brun, and J. Lotrian, Scattering through fluids: Speckle size measurement and Monte Carlo simulations close to and into the multiple scattering, Opt. Express **12**, 176 (2004).